Contrib Mineral Petrol (2001) 141: 347–357
DOI 10.1007/s004100100245

Francois Holtz · Andreas Becker · Marcus Freise
Wilhelm Johannes

The water-undersaturated and dry Qz-Ab-Or system revisited. Experimental results at very low water activities and geological implications

Received: 1 November 2000 / Accepted: 16 January 2001 / Published online: 11 April 2001

Abstract Liquidus phase relations have been determined in the system Qz-Ab-Or-H_2O at H_2O-undersaturated conditions (melt water content of 1 wt% H_2O) in the pressure range 200–800 MPa. Starting materials were homogeneous synthetic glasses containing 1 wt% H_2O. The minimum liquidus temperatures of the ternary system Qz-Ab-Or are 925 ± 15 °C at 200 MPa, 990 ± 10 °C at 500 MPa, and $1{,}050 \pm 10$ °C at 800 MPa. The normative Qz content of the minimum is 34 ± 2% at 200 MPa (the exact Ab/Or ratio could not be determined). The composition of the minimum is $Qz_{32}Ab_{35}Or_{33}$ at 500 MPa, and $Qz_{29}Ab_{37}Or_{34}$ at 800 MPa (Qz/Ab/Or expressed as normative proportions). At a given pressure, the Qz content of the minimum composition in the system Qz-Ab-Or-H_2O remains constant with changing a_{H2O}. The Qz content of the minimum composition increases with decreasing pressure and the normative Ab/Or ratio remains approximately constant (for a water content of the melt of 1 wt%). The determined liquidus temperatures in eutectic or minimum melts with 1 wt% H_2O, and the effect of pressure on the liquidus temperature are higher than estimated previously (ca. +0.2 °C/MPa between 200 and 800 MPa instead of less than +0.1 °C/MPa in previous estimations). Thus, at a given pressure, temperature and water content, the melt productivity in quartzofeldspathic rocks (such as metagreywackes) is lower than predicted from previous models. The experimental results show (1) that adiabatic decompression in the quartz-alkali feldspar system containing 0–3 wt% H_2O produces more melt than expected, which is of importance for the evolution of ascending dacitic and rhyolitic magmas, and (2) that previously published dry liquidus temperatures are strongly underestimated at high pressure (approximately 75 °C at 500 MPa).

F. Holtz (✉) · A. Becker · M. Freise · W. Johannes
Institut für Mineralogie, Universität Hannover,
Welfengarten 1, 30167 Hannover, Germany
E-mail: f.holtz@mineralogie.uni-hannover.de

Editorial responsibility: J. Hoefs

Introduction

The quaternary system SiO_2-$NaAlSi_3O_8$-$AlSi_3O_8$-H_2O (Qz-Ab-Or-H_2O) has received a great deal of attention from experimental petrologists over the last century. Much of this attention has been due to the interest generated by the fundamental studies of Schairer and Bowen (e.g., 1935), and Tuttle and Bowen (1958). The understanding of hydrous granite systems has achieved significant progress with the experimental results of Tuttle and Bowen (1958). Following this pioneering work, an impressive amount of studies have been undertaken to understand the effect of water on granite and quartz-feldspar phase relations (see reviews in Luth 1976; Johannes and Holtz 1996). However, the solubility mechanisms of water in granitic melts are still under debate (see reviews in McMillan 1994; Kohn 2000), and the most popular thermodynamic model for hydrous granitic systems (Burnham 1979) does not predict accurately the evolution of minimum compositions, water contents of melts and liquidus phase relationships as a function of water activity at pressures above 200 to 300 MPa (e.g., Montel and Vielzeuf 1997; Becker et al. 1998; Tamic et al. 2001).

Most experimental results on liquidus phase relations in the granite system Qz-Ab-Or ($Qz = SiO_2$; $Ab = NaAlSi_3O_8$; $Or = KAlSi_3O_8$) are obtained for "dry" and water-saturated conditions (e.g., dry compositions: Schairer and Bowen 1935; Schairer 1950; Luth 1969; water-saturated conditions: Tuttle and Bowen 1958; Luth et al. 1964; Merrill et al. 1970; Steiner et al. 1975). There have been several attempts to determine the "dry" solidus temperatures in the system Qz-Ab-Or (e.g., Huang and Wyllie 1975; Keppler 1989; Ebadi and Johannes 1991), but the dry minimum or eutectic melt compositions of the ternary system Qz-Ab-Or are not known at high pressures. Early experiments have shown that

equilibrium liquidus temperatures at dry conditions are difficult to obtain as a result of the high polymerization of dry melts. At one bar, Schairer and Bowen (1935) did not reach equilibrium in quartz-alkali feldspar compositions even in very long runs (up to 5 years). However, minimum melt or eutectic compositions in hydrous and anhydrous systems are key data needed for any further thermodynamic calculations (see, for example, Blencoe 1992; Holland and Powell 1998; Kirschen and Pichavant 2001).

One possible way to examine the effect of water on phase relations is to perform experiments at water-undersaturated conditions, with water contents which are high enough to allow equilibrium conditions to be reached (e.g., Clemens and Wall 1981). Such liquidus phase relations have been determined by Pichavant (1987), Holtz et al. (1992), and Pichavant et al. (1992) in the system Qz-Ab-Or-H_2O-CO_2. However, the extrapolation to almost "dry" conditions remained difficult because of the relatively high water contents in the investigated systems (> 2 wt% H_2O). Becker et al. (1998) worked out the liquidus phase relations at 500 MPa and $a_{H_2O} \approx 0.07$ (1 wt% H_2O in the melt), and their results suggest that the liquidus temperatures in water-poor systems are significantly shifted to higher temperatures when compared with previous estimations. In this study, phase relations in the haplogranitic system containing 1 wt% H_2O have been determined at 200 and 800 MPa. The results, combined with those at 500 MPa, are used to constrain the liquidus curves for minimum melt compositions at dry and strongly water-undersaturated conditions. This, in turn, is of importance for the calculation of the evolution of melt fractions in granitic systems as a function of P, T and water content.

Starting materials, experimental and analytical apparatus

The preparation of the starting material, the experimental apparatus, and the analytical techniques that have been used are described in detail by Becker et al. (1998). Only the most important points are summarized in this section.

The starting materials for the investigation of liquidus temperatures were crushed glasses (size < 200 μm) containing 1 wt% H_2O. For the realization of the experiments, the glass powders were placed into platinum capsules sealed at both ends. The synthesis of these hydrous glasses was conducted in three steps: (1) a mixture of oxides (SiO_2, Al_2O_3) and carbonates (Na_2CO_3, K_2CO_3) was heated at 1,600 °C for 24 h in a box furnace to produce dry glass batches of approximately 30 g; (2) these glasses were stirred at 1,600 °C for 5 days to obtain homogeneous crystal-free glasses; (3) mixtures of equal amounts of glass fragments with grain sizes of approximately 500 and 200 μm were sealed together with 1 wt% H_2O in Pt capsules, and subsequently heated in a gas-pressure vessel at 1,200 °C and 500 MPa for 120 h to produce a homogeneous hydrous glass. No particular care was taken to avoid an alkali loss during the stirring of the melt at 1,600 °C (step 2). Microprobe analyses showed that there were no concentration profiles along the synthesized dry glass blocks after step 2. The microprobe analyses of the 12 dry compositions are given in Table 1. The compositions do not depart significantly from the Qz-Ab-Or system, and have less

Table 1 Microprobe analysis and CIPW norms of dry starting glasses (average of at least eight analyses). The water content of the glasses after the hydration experiments is also given (*KFT* determined by Karl-Fischer titration, *IR* determined by infrared spectroscopy)

Glass no.	$Qz_{18.5}$ $Ab_{48.0}$ $Or_{33.3}$	σ	$Qz_{18.7}$ $Ab_{39.7}$ $Or_{41.5}$	σ	$Qz_{20.5}$ $Ab_{30.2}$ $Or_{48.9}$	σ	$Qz_{29.6}$ $Ab_{42.0}$ $Or_{28.1}$	σ	$Qz_{28.0}$ $Ab_{36.3}$ $Or_{35.7}$	σ	$Qz_{30.8}$ $A_{26.6}$ $Or_{42.4}$	σ	$Qz_{32.2}$ $Ab_{32.3}$ $Or_{31.8}$	σ	$Qz_{36.1}$ $Ab_{31.3}$ $Or_{32.6}$	σ	$Qz_{38.6}$ $Ab_{36.2}$ $Or_{25.1}$	σ	$Qz_{41.1}$ $Ab_{22.2}$ $Or_{36.2}$	σ
SiO_2	73.96	0.38	73.75	0.49	73.94	0.36	76.37	0.62	76.62	0.75	76.47	0.37	77.57	0.27	78.97	0.71	79.78	0.65	80.08	0.48
Al_2O_3	15.60	0.15	15.65	0.20	14.99	0.14	13.56	0.18	13.77	0.13	12.91	0.13	12.78	0.14	12.09	0.20	11.72	0.15	10.96	0.18
Na_2O	5.83	0.19	4.75	0.14	3.83	0.14	4.94	0.12	4.32	0.13	3.28	0.09	4.30	0.19	3.71	0.18	4.28	0.17	2.83	0.08
K_2O	5.69	0.18	7.10	0.24	8.37	0.17	4.74	0.09	6.09	0.17	7.15	0.22	5.38	0.09	5.54	0.14	4.25	0.15	6.14	0.19
Total	101.09		101.25		101.13		99.86		100.79		99.81		100.04		100.31		100.03		100.01	
Qz	18.51		18.71		20.49		29.61		27.98		30.75		32.29		36.10		38.62		41.14	
Ab	48.02		39.67		30.17		41.96		36.25		26.63		35.78		31.27		36.20		22.20	
Or	33.28		41.46		48.91		28.12		35.69		42.35		31.78		31.62		25.09		36.25	
C	0.00		0.15		0.00		0.30		0.08		0.00		0.00		0.00		0.09		0.00	
NaS	0.19		0.00		0.44		0.00		0.00		0.27		0.15		0.00		0.00		0.41	
Ks	0.00		0.00		0.00		0.00		0.00		0.00		0.00		0.00		0.00		0.00	
H_2O (KFT)	1.04		1.08		1.07		1.05		1.05		0.98		1.08		1.00		0.94		1.10	
H_2O (IR)	1.04		1.05		1.06												0.98		1.13	

than 0.6% normative corundum or metasilicate. The water contents of all glasses were determined by Karl Fischer titration (KFT; see analytical details in Behrens et al. 1996) and are given in Table 1. The distribution of water in five glass cylinders was also investigated by IR spectroscopy. The determined water contents are in agreement with KFT determinations, and water is distributed homogeneously in the samples (several sections along the glass cylinders show a variation in water content of less than 0.02 wt% H_2O).

The experiments were performed in a vertically oriented, internally heated gas-pressure vessel. The temperature gradients along the 10-mm-long platinum capsules are less than 2 °C (four K-type thermocouples were used). The temperature accuracy is estimated to be ± 5 °C. Pressure was measured using a tensile strength barometer with an accuracy of ± 100 bar. Heating and quenching were performed isobarically.

Experimental products were analyzed optically for the presence of quartz and/or feldspar crystals. Chemical compositions of minerals and melts were determined with a Camebax electron microprobe. Analytical conditions were 15 kV, 18 nA. Counting times for Na and K were 5 s for minerals, and 2 s for glasses. Counting times for Si and Al were 10 s for minerals, and 5 s for glasses.

Experimental procedure and reaction kinetics

The realization of experiments in almost dry granitic systems is notoriously difficult because strong undercooling may occur. To ensure that near-equilibrium conditions are reached at the investigated conditions (1 wt% water in the system), Becker et al. (1998) conducted several kinetic investigations. They tested (1) the influence of the grain size of the starting material, (2) the effect of the temperature path on nucleation and undercooling, and (3) the time needed to attain near-equilibrium compositions of the run products. The results support the experimental approach used by Pichavant (1987), and confirm that equilibrium liquidus temperatures are best approached in crystallization experiments using crushed glasses as starting materials which are directly brought to the run temperature. However, in contrast to Pichavant (1987), the experiments of Becker et al. (1998) and in this study were performed with hydrated glasses, and no H_2O-CO_2 fluid phase was coexsiting with the aluminosilicate phases (melt, or melt and crystals). A run duration of more than 168 h was found to be long enough to determine the liquidus temperature (for experimental and analytical results of kinetic studies, see Becker et al. 1998).

In addition to kinetic studies, the liquidus temperatures determined by Becker et al. (1998) were bracketed by crystallization and dissolution experiments for some key compositions (a detailed description of the procedure for dissolution experiments is given by Becker et al. 1998; see also Pichavant 1987). In crystallization experiments, the hydrated crushed starting glass is brought directly to the experimental temperature for 168 h. In these experiments, the experimental temperature is attained within 20 to 40 min. In dissolution experiments, samples were first brought 10–20 °C below the temperature of "first" crystallization (determined from crystallization experiments) for 72 h. Two capsules were always run simultaneously for this first step, one being opened to check for the presence of crystals. The second capsule was not opened, and was again heated up to a temperature 10 or 20 °C above the temperature of "first" crystallization and held here for 96 h. Becker et al. (1998) showed that the dissolution experiments confirmed the liquidus temperatures determined from crystallization experiments within a temperature interval of 10 °C in quartzofeldspathic melts containing 1 wt% H_2O. Thus, in this study the realization of dissolution experiments, which is more time consuming and which requires twice as many Pt capsules, was not performed systematically. In one experiment at 800 MPa with composition $Qz_{28.0}Ab_{36.3}Or_{35.7}$, the liquidus temperature between 1,060 and 1,040 °C could be reproduced with a dissolution experiment (run 642; see below). Because of the temperature steps chosen in this study, the liquidus temperatures are only bracketed within 20 °C.

Results

Experimental products consisted of glass or glass and crystals (crystals: quartz and alkali feldspars). The results of crystallization experiments performed with crushed hydrous starting materials and relevant for the determination of liquidus temperatures are given in Tables 2 and 3 (results at 200 and 800 MPa, respectively). For temperatures which are 10–20 °C below the liquidus temperature, feldspars are "tabular" and quartz shows the typical bipyramidal shape (for typical products, see Figs. 6 and 7 in Becker et al. 1998). The run product of the dissolution experiment (run 642 in Table 3) consisted of glass only. The phase relationships

Table 2 Experimental results at 200 MPa, 1 wt% H_2O in the system Qz-Ab-Or-H_2O (*gl* Glass, *fsp* Feldspar, *qtz* Quartz)

Experiment no.	Starting glass	(Or/Or + Ab)100	Temperature (°C)	Run duration (h)	Products (Observed phases)
672	$Qz_{18.5}Ab_{48.00}Or_{33.3}$	40.9	960	96	fsp + gl
678			980	96	gl
668	$Qz_{20.5}Ab_{30.2}Or_{48.9}$	61.8	960	96	fsp + gl
677			980	96	gl
697	$Qz_{29.6}Ab_{42.0}Or_{28.1}$	40.1	920	120	fsp + qtz + gl
706			940	120	fsp + gl
716			960	120	gl
710	$Qz_{32.3}Ab_{35.8}Or_{31.8}$	47.0	940	120	fsp + gl
717			960	120	gl
696	$Qz_{30.8}A_{26.6}Or_{42.4}$	61.4	920	120	fsp + qtz + gl
707			940	120	fsp + gl
714			960	120	gl
694	$Qz_{28.0}Ab_{36.3}Or_{35.7}$	49.6	920	120	fsp + qtz + gl
705			940	120	fsp + gl
712			960	120	gl
702	$Qz_{36.1}Ab_{31.3}Or_{32.6}$	51.1	920	120	fsp + qtz + gl
711			940	120	fsp + gl
718			960	120	gl

Table 3 Experimental results at 800 MPa, 1 wt% H_2O in the system Qz-Ab-Or-H_2O (all runs are crystallization experiments except run 642 which is a two-step (crystallization followed by dissolution) reverse experiment; run 641 is a control experiment to check the phase assemblage obtained after the first step of run 642; *gl* Glass, *fsp* Feldspar, *qtz* Quartz)

Experiment no.	Starting glass	(Or/Or + Ab)100	Temperature (°C)	Run duration (h)	Products (Observed phases)	Or in alk. fsp (wt%)
625	$Qz_{18.5}Ab_{48.00}Or_{33.3}$	40.9	1,060	168	fsp + gl	34.7
610			1,080	168	gl	
611	$Qz_{18.7}Ab_{39.7}Or_{41.5}$	51.1	1,080	168	fsp + gl	52.1
651			1,100	168	gl	
612	$Qz_{20.5}Ab_{30.2}Or_{48.9}$	61.8	1,080	168	fsp + gl	68.4
652			1,100	168	gl	
618	$Qz_{29.6}Ab_{42.0}Or_{28.1}$	40.1	1,060	172	fsp + qtz + gl	29.8
613			1,080	168	gl	
629	$Qz_{32.3}Ab_{35.8}Or_{31.8}$	47.0	1,060	168	fsp + qtz + gl	40.2
630			1,080	120	gl	
604	$Qz_{28.0}Ab_{36.3}Or_{35.7}$	49.6	1,040	168	fsp + qtz + gl	50.5
619			1,060	172	gl	
641			1,020	72	fsp + qtz + gl	
642 Crys. →Diss			1,020→1,060	72→96	gl	
620	$Qz_{30.8}A_{26.6}Or_{42.4}$	61.4	1,060	172	fsp + qtz + gl	67.55
615			1,080	168	gl	
663	$Qz_{36.1}Ab_{31.3}Or_{32.6}$	51.1	1,140	168	qtz + gl	
658			1,160	168	gl	
664	$Qz_{38.6}Ab_{36.2}Or_{25.1}$	48.9	1,200	168	qtz + gl	
665	$Qz_{41.1}Ab_{22.2}Or_{36.2}$	61.0	1,200	168	qtz + gl	

of the ternary system Qz-Ab-Or at 200 and 800 MPa are shown in Figs. 1 and 2, respectively. The isotherms are fixed by results of crystallization experiments with either quartz or feldspar coexisting with the melt (Tables 2 and 3), and by the composition of these phases at 800 MPa (see Table 4 for compositions of feldspars and glasses).

At 200 MPa, the crystals were too small to be analyzed, and only qualitative information could be obtained from the microprobe analyses. However, the

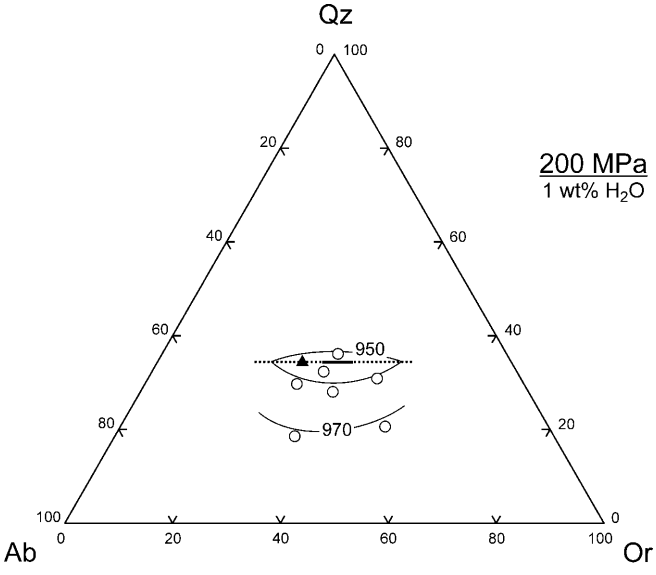

Fig. 1 Triangular diagram showing liquidus phase relationship of the system Qz-Ab-Or-H_2O at 200 MPa (1 wt% H_2O in the melt), projected onto the anhydrous system Qz-Ab-Or. *Open circles* Composition of the starting glasses. *Dotted line* Projected cotectic curve. *Continuous section along dotted line* Most probable compositional range of the minimum composition. *Continuous lines labeled 950 and 970* Isotherms (in °C) on the liquidus surface. *Closed triangle* Water-saturated minimum at 200 MPa (Tuttle and Bowen 1958; see data in Table 5)

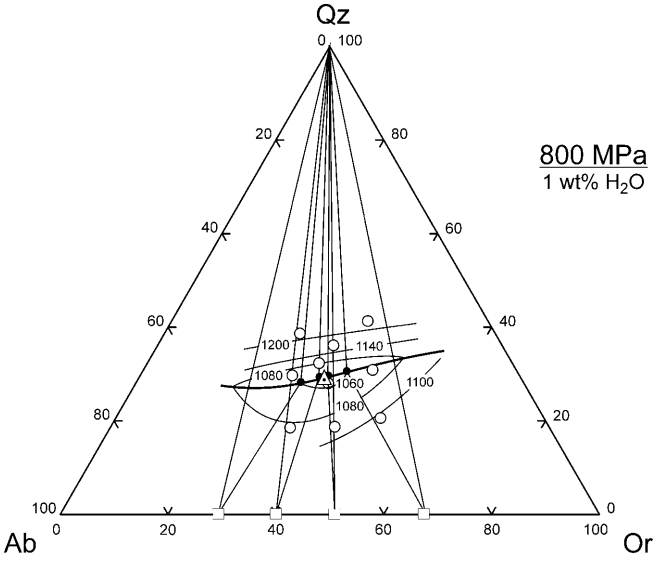

Fig. 2 Triangular diagram showing liquidus phase relationship of the system Qz-Ab-Or-H_2O at 800 MPa (1 wt% H_2O in the melt). *Open circles* Composition of the starting glasses. *Closed circles* Compositions of melts connected by conjugation lines with coexisting quartz and feldspar. *Open squares* Feldspar composition for the three phase assemblages. *Thick line* Projected cotectic curve. *Lines labeled 1060, 1080,* etc. Isotherms (in °C) on the liquidus surface. The anhydrous composition of the minimum shown by the triangle is $Qz_{29}Ab_{37}Or_{34}$

Table 4 Microprobe analysis of glasses (melts) and coexisting alkali feldspars obtained from crystallization experiments in the system Qz-Ab-Or-H_2O (averages of at least eight analyses; structural formulae on the basis of eight oxygen atoms) at 800 MPa

Experiment no.	625	611	612	618	629	604	620	663	664	665
Temperature (°C)	1,060	1,080	1,080	1,060	1,060	1,040	1,060	1,140	1,200	1,200
Composition of partial melts										
SiO_2	74.01	72.84	73.57	75.77	75.23	75.22	74.15	78.06	74.86	78.92
Al_2O_3	14.28	14.20	13.66	13.47	13.02	13.45	13.89	12.29	13.53	11.40
Na_2O	5.03	4.53	3.93	4.85	4.57	4.11	4.63	3.97	4.45	2.96
K_2O	5.33	6.08	6.88	5.05	5.45	5.68	5.78	5.58	5.73	6.15
Total	98.65	97.65	98.04	99.13	98.27	98.46	98.45	99.91	98.57	99.42
Qz	24.66	23.83	25.62	28.49	29.47	30.04	31.36	34.47	37.75	38.76
Ab	43.15	39.21	32.60	41.39	37.27	35.34	31.54	32.16	37.68	24.53
Or	31.96	36.78	41.47	30.08	32.79	34.07	36.95	33.03	24.27	36.54
C	0.23	0.18	0.00	0.03	0.00	0.55	0.00	0.00	0.29	0.00
NaS	0.00	0.00	0.30	0.00	0.48	0.00	0.15	0.34	0.00	0.16
KS	0.00	0.00	000	0.00	0.00	0.00	0.00	0.00	0.00	000
Composition of alkali feldspars										
SiO_2	68.34	67.19	66.35	68.27	68.38	68.44	67.86			
Al_2O_3	18.70	18.52	18.15	19.39	18.30	17.99	18.46			
Na_2O	7.39	5.53	3.60	8.17	6.57	5.54	5.97			
K_2O	5.63	8.60	11.13	4.97	6.33	8.10	7.63			
Total	100.07	99.84	99.22	100.80	99.59	100.07	99.92			
Si	3.03	3.02	3.03	3.00	3.05	3.05	3.03			
Al	0.98	0.98	0.98	1.00	0.96	0.95	0.97			
Na	0.66	0.50	0.33	0.72	0.59	0.50	0.54			
K	0.32	0.49	0.65	0.28	0.36	0.46	0.44			

presence or absence of quartz and feldspars could be clearly confirmed by optical techniques. Back-scattered electron images showed that the nucleation of minerals mostly occurred at the boundaries of the former glass grains. Because of the low amounts of crystals, which is probably related to nucleation and kinetic problems (crystal growth rate) at low pressure, the glass composition did not change significantly in experimental products containing crystals. Thus, the composition of the minimum at 200 MPa is only constrained by the observed mineral assemblage and the liquidus temperatures of the investigated bulk compositions, but not by the compositions of the experimental products. Because several starting compositions close to that of the presumed minimum were used, the position of the cotectic line and the Qz content of the minimum are relatively well constrained. The phase diagram in Fig. 1, resulting from the data in Table 2, shows that the cotectic line lies between the compositions $Qz_{36.1}Ab_{31.3}Or_{32.6}$ and $Qz_{32.3}Ab_{35.8}Or_{31.8}$. Thus, the normative Qz content of the minimum composition is 34 ± 2 wt%. All three phase assemblages were found to occur in the temperature interval 940–920 °C, and the minimum liquidus temperature was estimated to be 925 ± 15 °C. It has to be noted that this temperature is a minimum temperature because the liquidus temperature would be higher if undercooling occurred in the 200-MPa experiments (see nucleation problems mentioned above). The Ab/Or ratio of the minimum composition is difficult to determine because the feldspar phases in the ternary assemblages were too small to be analyzed. As a result, the conjugation lines which are helpful to constrain the minimum composition could not be drawn. The possible compositional range in which the minimum composition must be located is marked in Fig. 1 (part of the cotectic line marked by a continuous line). For comparison, the water-saturated minimum composition has also been reported (closed triangle in Fig. 1).

At 800 MPa, the sizes of the feldspar crystals were 3–50 μm, and those of quartz were < 5 μm. Eight to ten crystals were analyzed in experimental products containing feldspars. As expected, the compositions of the glasses coexisting with quartz or feldspar (Table 4) are always shifted toward the composition of the cotectic line. In four crystallization experiments, quartz and alkali feldspar coexist with the melt (Table 3). The composition of these melts and the corresponding temperatures are used to constrain the position of the cotectic line (see triangles connecting the compositions of feldspar, quartz and glass in Fig. 2). The position of the cotectic line at 800 MPa is well constrained by these four experiments (Table 3, runs 618, 629, 604, 620). The composition of the minimum is tightly constrained by two melt compositions (from runs 604 and 629). The composition and temperature of the ternary minimum is $Qz_{29}Ab_{37}Or_{34}$ (normative proportions) and $1{,}050 \pm 10$ °C (1 wt% H_2O in the system).

Discussion

Individual effects of P and water activity on minimum composition

The data available in the literature on the compositions and temperatures of minima determined at various

Table 5 Composition (normative proportions), temperature at the liquidus, and water content of the minimum and eutectic points in the system Qz-Ab-Or-H_2O-(CO_2). *n.d.* Not determined, *wat.-sat.* water-saturated conditions, *CO_2* water-undersaturated conditions with a H_2O-CO_2 fluid phase

Pressure (MPa)	Normative Oz-Ab-Or	Water content (wt%)	Temperature (°C)	Source of data[a]	Remarks
200	35/39/26	n.d.	685	1	Wat.-sat.
200	36/39/25	5.8	685	2, 3	Wat.-sat.
200	35/36/29	3.6	775	2, 3	CO_2
200	35/34/31	2.3	830	2, 3	CO_2
200	34/n.d./n.d.	1.0	925	This study	Fluid-absent
500	31/47/22	9.9	645	2, 3	Wat.-sat.
500	32/43/25	5.9	735	2, 3	CO_2
500	32/40/28	4.3	790	2, 3	CO_2
500	32/35/33	1.0	990	4	Fluid-absent
800	29/37/34	1.0	1,050	This study	Fluid-absent

[a]Data sources are *1* Tuttle and Bowen (1958), *2* Holtz et al. (1992), *3* Holtz et al. (1995), *4* Becker et al. (1998) and this study

water activities and at 200, 500 and 800 MPa are summarized in Table 5. At 200 and 500 MPa, the Qz content of the minimum determined for 1 wt% H_2O in the melt is practically identical to that determined at the same pressures for water-saturated and water-undersaturated conditions (Tuttle and Bowen 1958; Holtz et al. 1992). The Ab/Or ratio of the minimum decreases with decreasing water content of the melt, in agreement with previous studies (e.g., Pichavant 1987; Holtz et al. 1992; Becker et al. 1998). Data at 800 MPa are only available for 1 wt% H_2O in the system, and the effect of water activity can not be determined clearly at this pressure.

The data at 500 and 800 MPa allow us to estimate the effect of increasing pressure on the composition of the minimum at a constant water content of the melt. The Qz content of the minimum composition decreases at approximately constant Ab/Or ratio with increasing pressure.

In most experiments performed at water-undersaturated conditions, a C-H-O fluid phase was used to reduce the water activity (e.g., Kesson and Holloway 1974; Clemens and Wall 1981; Pichavant 1987; Ebadi and Johannes 1991; Holtz et al. 1992; Pichavant et al. 1992). All these experiments were carried out at relatively oxidizing conditions, and the fluid phase is mainly composed of CO_2 and H_2O. It has been suggested that the effect of water on liquidus phase relationships described by Holtz et al. (1992) and Pichavant et al. (1992) in the quartzofeldspathic system may result from the combined effects of decreasing H_2O and increasing CO_2 contents of the melt (Nekvasil and Carroll 1996), and that CO_2 may play an independent part in the modification of phase equilibria. The comparison of results obtained for a CO_2-free system in this study with the results obtained by Holtz et al. (1992) in CO_2-bearing systems demonstrates that CO_2 dissolved in quartzofeldspathic melts at 200 and 500 MPa does not measurably affect the phase relationships. It is emphasized that, at the conditions at which the experiments were performed, the stable C-bearing species which is dissolved in granitic or quartzofeldspathic melts is molecular CO_2 (e.g., Blank et al. 1993; Blank and Brooker 1994; Tamic et al. 2001), and that the solubility remains low (maximal solubility is less than 2,500 ppm at 500 MPa; Fogel and Rutherford 1990; Tamic et al. 2001).

Liquidus curve for 1 wt% water and "dry" liquidus curve

The experimental results can be used to constrain the liquidus P-T conditions for minimum or eutectic compositions containing 1 wt% H_2O. The liquidus curve for 1 wt% H_2O is shown in Fig. 3 and is constrained by the experimental data at 200, 500 and 800 MPa and by water solubility data obtained at very low pressure for a rhyolitic melt (Yamashita 1999). Although this natural rhyolitic composition is not identical to the minimum composition at low pressure in the quartzofeldspathic system, a difference in water solubility between the rhyolitic and minimum quartzofeldspathic compositions of more than 5% relative is not expected (Behrens and Jantos 2001). Using the experimental results constraining the temperature of the water-saturated solidus curve (Ebadi and Johannes 1991) and the water solubility at low pressure (Yamashita 1999), a water solubility of 1 wt% H_2O along the water-saturated solidus curve is obtained at approximately 12 MPa and 875 °C.

Figure 3 shows that the neither the slope nor the location of the liquidus curve for 1 wt% H_2O can be reconciled with previous data obtained at dry conditions. For example, the minimum temperature at 500 MPa for a water content of the melt of 1 wt% H_2O (990 ± 10 °C) is very close or identical to that obtained at "nominally dry" conditions (1,010 °C in Huang and Wyllie 1975; 1,000 °C in Ebadi and Johannes 1991). The liquidus temperature at 800 MPa for 1 wt% H_2O in the melt is even 10 °C higher than the "nominally dry" liquidus determined previously. As demonstrated by Becker et al. (1998), this discrepancy results from the presence of minor amounts of water in the experimental charges in the experiments at "nominally dry" conditions, which can have dramatic effects on the estimation of liquidus temperatures. The previous "dry" liquidus curve was constrained by solidus experiments. In such

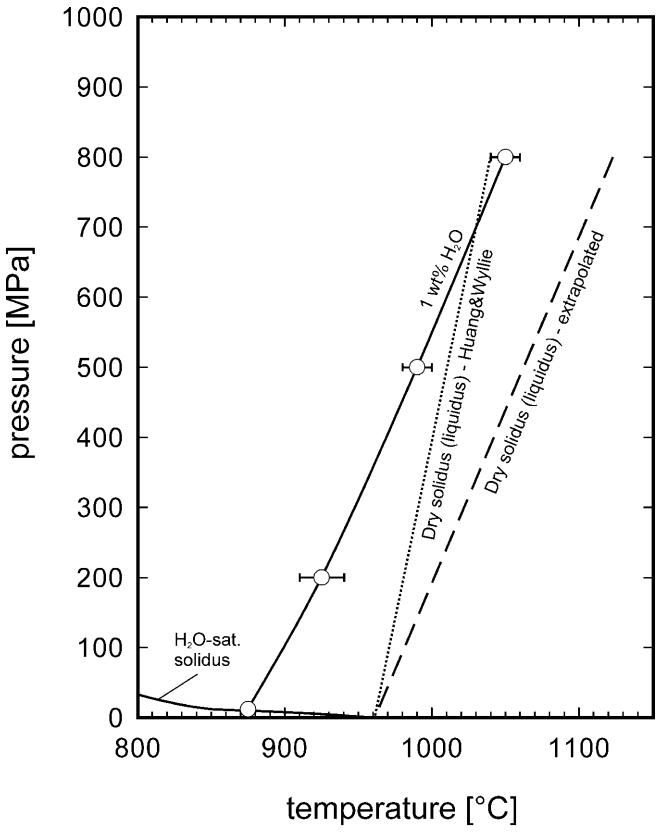

Fig. 3 Water-saturated solidus curve and liquidus curves for 1 and 0 wt% H_2O in the system Qz-Ab-Or. *Continuous line* Liquidus curve for 1 wt% H_2O determined in this study (at 200, 500, 800 MPa) and from water-solubility data of Yamashita (1999; cf. *open circles* on the water-saturated solidus curve). *Dotted line* "Dry" solidus curve from Huang and Wyllie (1975) which corresponds also to the "dry" liquidus curve for the minimum composition. *Dashed line* Estimated new dry solidus curve and liquidus curve for the minimum composition (for further explanation, see text)

experiments, the starting material was an assemblage of quartz and feldspars. Run products in which melt was detected were used to bracket the dry solidus curve, which represents also the liquidus curve if the initial mineral assemblage corresponds to the minimum composition. In such "nominally dry" solidus experiments, the presence of very small amounts of free interstitial water will lead to the formation of melt, which can result in an underestimation of the dry solidus and liquidus temperature. In addition, these solidus experiments were performed with a piston cylinder apparatus. In such an apparatus with solid pressure media, it has recently been shown that water can move from the solid pressure medium through platinum noble-metal capsules into the sample (Patino Douce and Beard 1994; Truckenbrodt and Johannes 1999), which may also influence the determined solidus temperatures, especially at temperatures above 1,050 °C.

It is therefore concluded that the position and slope of the liquidus curve for dry conditions needs to reconsidered. Although this curve is not interesting for geologically relevant conditions, it gives boundary conditions needed to be known for thermodynamic or empirical modeling (e.g., Margules approach, models involving non-ideal mixing properties). A possible location of the dry liquidus curve in the P-T field is shown in Fig. 3. This new dry liquidus curve has been constrained from the evolution of the temperature of the liquidus (for minimum or eutectic compositions) with decreasing water content of the melt (decreasing water activity) at 500 and 200 MPa (see Fig. 4). Two different and independent data sets have been used to draw the two curves in Fig. 4: (1) the liquidus phase relationships in the haplogranitic system for given water content of the melt (Holtz et al. 1992, and this study; see data in Table 5), and (2) the combination of water-solubility data and solidus temperatures obtained for systems in equilibrium with C-H-O fluid phases. In the latter case the water solubility in the silicate melt for a given XH_2O in the fluid has been calculated at the solidus temperature of a quartzofeldspathic assemblage coexisting with a fluid having the same XH_2O. The solidus temperature and the calculated melt water content correspond to those of the minimum composition for a given water activity constrained by the XH_2O of the fluid. The water-solubility model of Tamic et al. (2001) for natural rhyolitic melts coexisting with H_2O-CO_2 fluids, and the solidus temperatures for the quartzofeldspathic system determined at 200 MPa ($XH_2O = 0.08$ and 0.26) and 500 MPa ($XH_2O = 0.06$ and 0.22) by Ebadi and Johannes (1991) have been used, the corresponding H_2O

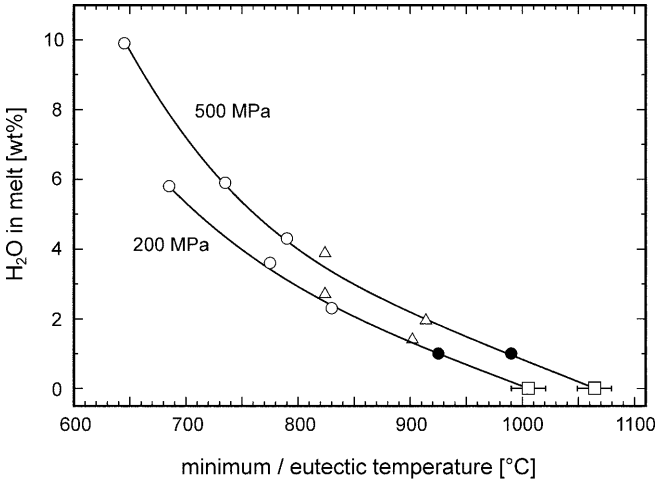

Fig. 4 Diagram showing the evolution of the minimum temperatures in the system Qz-Ab-Or-H_2O at 200 and 500 MPa as a function of the water content of the melt. *Shaded circles, open circles, closed circles* Experimental data obtained from liquidus phase relationships in the system Qz-Ab-Or at water-saturated conditions, moderately water-undersaturated conditions (Holtz et al. 1992), and strongly water-undersaturated conditions (with 1 wt% H_2O, this study), respectively. *Triangles* Data calculated using the solidus curves and the water-solubility values for known XH_2O (see text). The curves have been used to estimate the temperature of the dry liquidus in this system (*squares*)

content/temperature combinations being indicated by triangles in Fig. 4. The water content of the melt at water-saturated conditions and at the water-saturated solidus temperature (shaded circles in Fig. 4) are from Holtz et al. (1995). The extrapolation of the curves in Fig. 4 toward a water content of the melt of 0 wt% (by an empirical "best fit") allows us to estimate the dry liquidus temperature to be approximately 1,005 and 1,065 °C at 200 and 500 MPa, respectively. It can be noted that these temperatures are probably minimum temperatures, because this extrapolation is not expected to overestimate the dry liquidus temperature – it is well known that the effect of water on phase relations and physical properties of aluminosilicate melts is nonlinear and more pronounced at lower water content of the melt. The dry liquidus curve in Fig. 3 was drawn assuming a linear fit between the dry liquidus temperature of 960 °C at 1 bar (Tuttle and Bowen 1958), and the estimated dry liquidus temperatures of 1,005 and 1,065 °C at 200 and 500 MPa, respectively.

Liquidus curves for a given amount of water in the system (for minimum and eutectic quartzofeldspathic compositions)

The new positions of the liquidus curves for 1 wt% water and for dry conditions determined in this study allow us to draw a new set of liquidus curves for given amounts of water in the melt (Fig. 5). It is emphasized that the liquidus is only attained at the given P, T, and H_2O content of the melt if its composition corresponds to that of the minimum (or eutectic point) in the system Qz-Ab-Or-H_2O. The new liquidus curves shown in Fig. 5 have been constructed from different data sets.

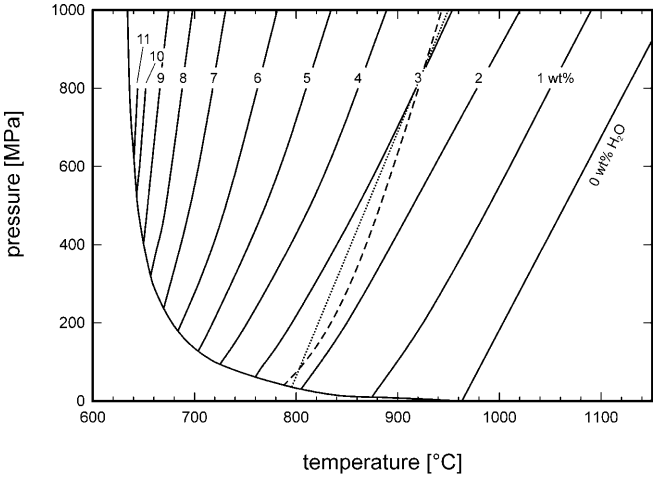

Fig. 5 Water-saturated solidus curve and liquidus curves for given amounts of H_2O in the system Qz-Ab-Or-H_2O. *Continuous lines* New liquidus curves determined in this study. *Dotted line* Liquidus curve for melts containing 2 wt% H_2O from the model of Clemens and Vielzeuf (1987). *Dashed line* Liquidus curve for quartzofeldspathic compositions containing 2 wt% H_2O published by Johannes and Holtz (1996). The liquidus curves indicate the minimum water contents which need to be dissolved in melts having a minimum or eutectic composition at given P and T. For example, a quartzofeldspathic minimum composition containing 3 wt% water or more will be completely melted at 920 °C and 800 MPa. If 1 wt% water is present in the system at the same P-T conditions, the stable assemblage will be composed of 33.33 wt% melt containing 3 wt% H_2O and 66.67 wt% anhydrous crystals

1. The minimum liquidus temperatures in the system Qz-Ab-Or-H_2O at water-undersaturated conditions for given water contents of the melt (see data in Table 5). These temperatures correspond to the "minimum melt" temperatures determined from liquidus phase relationships (such as those published for water-saturated conditions in the pioneering work of Tuttle and Bowen 1958). Each liquidus phase diagram established for a given pressure and water activity (such as the diagram in Fig. 2) gives information only for the location of one point in the P-T diagram of Fig. 5 (such points are represented by the circles at 200, 500 and 800 MPa in Fig. 3). However, such liquidus phase diagrams represent the only experimental way to directly constrain P, T, and the minimum water content of first melts (formed from a quartzofeldspathic assemblage) from the same experimental data set. Because of the considerable amount of experiments necessary to determine the liquidus phase relationships at a given water activity and pressure, such data are scarce (see Table 5).

2. The water solubility in silicate melts along the water-saturated solidus curve. At the temperature of the water-saturated solidus and for a minimum or eutectic melt composition in the system Qz-Ab-Or-H_2O, the water content of the melt constrained by the water-solubility curve (equilibrium curve: melt/melt + vapor) is identical to the water content of the melt at the liquidus (equilibrium curve: melt/melt + crystals; see, for example, Fig. 1 in Holtz et al. 2001). For example, if a water solubility of 9 wt% H_2O is observed at 400 MPa at the solidus temperature (approximately 645 °C; Fig. 5), the liquidus curve for the quartzofeldspathic minimum composition with 9 wt% H_2O will necessarily end at this point. To improve the geological relevance of the liquidus curve, the water-solubility data for natural rhyolitic or leucogranitic melts have been used when possible to draw the curves in Fig. 5 (data from Silver et al. 1990, and Behrens and Jantos 2001 at P between 500 and 50 MPa; Yamashita 1999 at $P < 50$ MPa; for calculation of water solubility, see Holtz et al. 2001). As emphasized above, the water solubility in rhyolitic melts does not deviate by more than 5% relative from the water solubility of minimum melt compositions in the system Qz-Ab-Or (Behrens and Jantos 2001).

3. The combination of solidus curves (Ebadi and Johannes 1991) and water-solubility curves in quartzofeldspathic melts for given mole fractions of water in a coexisting H_2O-CO_2 fluid (Tamic et al. 2001). This procedure has also been used to constrain the dry liq-

uidus temperature (see above). It is emphasized that this method was only used to calculate water contents of the melts for P-T conditions of 75–500 MPa and 800–1,100 °C (limit of application of the empirical water-solubility model of Tamic et al. 2001).

It can be noted that the location of the liquidus curves shown in Fig. 5 has been modeled successfully by Kirschen and Pichavant (2001), based on the Margules approach. The agreement between the liquidus curves resulting from the thermodynamic modeling (Kirschen and Pichavant 2001) and from the empirical fit of experimental data (this study) is not surprising because the water-solubility data and the experimental phase relationships used in the present study have also been used to constrain solution parameters by Kirschen and Pichavant (2001). However, to our knowledge, this thermodynamic model is the first which reproduces correctly the experimental phase equilibria of the quartzofeldspathic system as a function of water activity (at least in the pressure range 200–500 MPa).

Geological implications

Although natural protoliths have never exactly the mineral assemblage corresponding to the quartzofeldspathic minimum, the liquidus curves shown in Fig. 5 are important in understanding melting processes because they indicate the minimum amount of water which can be dissolved in melts at given P and T (e.g., Burnham 1979; Clemens and Vielzeuf 1987; Johannes and Holtz 1996). The new position of the liquidus curves determined in this study has several major geological implications.

1. Because the effect of pressure on the liquidus temperature of systems containing low amounts of water is higher than previously estimated, the increase of melt fraction due to adiabatic decompression is higher than predicted from the model of Clemens and Vielzeuf (1987) or the liquidus curves in Johannes and Holtz (1996). Compared with the liquidus curves and calculations of Johannes and Holtz (1996), the increase in melt fraction is approximately two times higher if decompression occurs at $T > 820$ °C. In contrast to previous liquidus curves (Clemens and Vielzeuf 1987; Johannes and Holtz 1996), it can be noted that the new curves have different slopes at low and high water contents. This indicates that the effect of dissolved water on phase relationships is different in systems with high and low water contents, which is consistent with the existence of different water species which are incorporated in different amounts and ratios at high and low water contents (at low water content, the proportion of hydroxyl groups to molecular water is higher than at high water content; e.g., Stolper 1982; Nowak and Behrens 1995; Shen and Keppler 1995).

2. Assuming a quartzofeldspathic protolith such as metagreywackes or fertile metapelites, the liquidus curves can be used to determine the minimum water content which can be incorporated in the melts at the appropriate P-T conditions (e.g., Holtz et al. 2001). The new position of the liquidus curves for low water contents implies that, for conditions above 800 °C and in the pressure range 400–800 MPa, which are representative for anatectic conditions of many granitic melts, the water contents of melts derived from the partial melting of pelitic or quartzofeldsdpathic rocks will be significantly higher than previously assumed. In the P-T field mentioned above, the water content of the melts are underestimated by approximately 25–35% if the data sets obtained from Clemens and Vielzeuf (1987), and Johannes and Holtz (1996) are used (see liquidus curves for 2 wt% H_2O of these authors in Fig. 5). This is in agreement with Montel and Vielzeuf (1997) who also noted that the water contents of melts produced from metagreywackes are higher than those predicted by the thermodynamic model of Burnham and Nekvasil (1986), and Nekvasil (1988). This observation is of importance because the water content of melts influences both the chemical (e.g., melt fraction, see below) and physical properties (e.g., viscosity) of magmas. In particular, it can be shown that the viscosity of melts containing minimum amounts of water is almost constant (± 0.5 log units) independently of the melting temperature, because the effect of water is almost exactly counterbalanced by that of temperature (Holtz et al. 2001). Thus, the new liquidus data set explains why the viscosity of melts migrating through the crust is found to be almost constant (Scaillet et al. 1998).

3. When compared to previous liquidus curves, the higher liquidus temperature for a given water content in the system has implications for the amount of melt which can be generated in the crust. In quartzofeldspathic rocks such as metagreywackes, the melt fraction is controlled by the bulk composition (e.g., Patino Douce and Johnston 1991), the mineralogical composition and the amount of water available for melting (especially in the case of dehydration melting reactions), and the minimum amount of water which is incorporated in the melts (e.g., Clemens and Vielzeuf 1987; Johannes and Holtz 1996). This study shows that, at high temperature, the minimum amounts of water are higher than previously assumed. For example, at 800 MPa and 920 °C, previous studies predicted a water content of the melt of 2 wt% (Fig. 5), whereas 3 wt% is expected from the new liquidus curves in Fig. 5. Assuming that 1 wt% is available to form melt at these conditions, a melt fraction of 33 wt% could be produced from a quartzofeldspathic rock, instead of 50%. As a consequence, the melt fractions which can be produced from a quartzofeldspathic source rock are significantly overestimated (up to 25 wt% relative at temperatures above 800 °C) if the model of Burnham (1979; see Clemens and Vielzeuf 1987) or the liquidus curves published by Johannes and Holtz (1996) are used to determine the minimum amounts of water dissolved in

melts. This is in agreement with studies on experimental melting of natural rock systems, in which the observed melt fractions were consisctently lower than the predictions of these former models (e.g., Patino Douce and Johnston 1991; Patino Douce and Beard 1995; Springer and Seck 1997).

Acknowledgements This work was supported by the German Science Foundation (DFG Az. Jo 63/64). We are grateful to O. Diedrich and W. Hurkuck for their technical assistance. The paper benefited from the comments of A. Patino Douce and an anonymous reviewer.

References

Becker A, Holtz F, Johannes W (1998) Liquidus temperatures and phase compositions in the system Qz-Ab-Or at 5 kbar and very low water activities. Contrib Mineral Petrol 130:213–224

Behrens H, Jantos N (2001) The effect of anhydrous composition on water solubility in granitic melts. Am Mineral 86:14–20

Behrens H, Romano C, Nowak M, Holtz F, Dingwell DB (1996) Near-infrared spectroscopic determination of water species in glasses of the system $MAlSi_3O_8$ (M = Li,Na,K): an interlaboratory study. Chem Geol 128:41–63

Blank GB, Brooker RA (1994) Experimental studies of carbon dioxide in silicate melts: Solubility, speciation, and stable carbon isotope behavior. Mineral Soc Am. Rev Mineral 30:157–186

Blank JG, Stolper EM, Carroll MR (1993) Solubility of carbon dioxide and water in rhyolitic melt at 850°C and 750 bars. Earth Planet Sci Lett 119:27–36

Blencoe JG (1992) A two-parameter Margules method for modelling the thermodynamic mixing properties of albite-water melts. Trans R Soc Edinb, Earth Sci 83:423–428

Burnham CW (1979) The importance of volatile constituents. In: Yoder HS Jr (ed) The evolution of the igneous rocks. Princeton University Press, Princeton, pp 439–482

Burnham CW, Nekvasil H (1986) Equilibrium properties of granite pegmatite magmas. Am Mineral 71:239–263

Clemens JD, Vielzeuf D (1987) Constraints on melting and magma production in the crust. Earth Planet Sci Lett 86:287–306

Clemens JD, Wall VJ (1981) Origin and crystallization of some peraluminous (S-type) granitic magma. Can Mineral 19:111–131

Ebadi A, Johannes W (1991) Beginning of melting and composition of first melts in the system Qz–Ab–Or–H_2O–CO_2. Contrib Mineral Petrol 106:286–295

Fogel RA, Rutherford MJ (1990) The solubility of carbon dioxide in rhyolitic melts: a quantitative FTIR study. Am Mineral 75:1311–1326

Holland TJB, Powell R (1998) An internally-consistent thermodynamic data set for phases of petrological interest. J Metamorph Geol 16:309–343

Holtz F, Pichavant M, Barbey P, Johannes W (1992): Effects of H_2O on liquidus phase relations in the haplogranite system at 2 and 5 kbar. Am Mineral 77:1223–1241

Holtz F, Behrens H, Dingwell DB, Johannes W (1995) Water solubility in haplogranitic melts. Compositional, pressure and temperature dependence. Am Mineral 80:95–108

Holtz F, Johannes W, Tamic N, Behrens H (2001) Maximum and minimum water contents of granitic melts generated in the crust: a reevaluation and implications. Lithos 56:1–14

Huang WL, Wyllie PJ (1975) Melting reactions in the system $NaAlSi_3O_8$–$KAlSi_3O_8$–H_2O to 35 kilobars, dry and with excess water. J Geol 83:737–748

Johannes W, Holtz F (1996) Petrogenesis and experimental petrology of granitic rocks. Springer, Berlin Heidelberg New York

Keppler H (1989) The influence of the fluid phase composition on the solidus temperatures in the haplogranite system $NaAlSi_3O_8$–$KAlSi_3O_8$–SiO_2–H_2O–CO_2. Contrib Mineral Petrol 102:321–327

Kesson SE, Holloway JR (1974) The generation of N_2-CO_2-H_2O fluids for use in hydrothermal experimentation II. Melting of albite in multispecies fluid. Am Mineral 59:598–603

Kirschen M, Pichavant M (2001) A thermodynamic model for hydrous silicate melts in the system $NaAlSi_3O_8$–$KAlSi_3O_8$–Si_4O_8–H_2O. Chem Geol 174:103–114

Kohn SC (2000) The dissolution mechanisms of water in silicate melts; a synthesis of recent data. Mineral Mag 64:389–408

Luth WC (1969) The system $NaAlSi_3O_8$–SiO_2 and $KAlSi_3O_8$–SiO_2 to 20 kbar and the relationship between H_2O content, P-H_2O, and P-total in granitic magmas. Am J Sci 267–A:325–341

Luth WC (1976) Granitic rocks. In: Bailey DK, MacDonald R (eds) The evolution of crystalline rocks. Academic Press, London, pp 335–417

Luth WC, Jahns RH, Tuttle OF (1964) The granite system at pressure of 4 to 10 kilobars. J Geophys Res 69:759–773

McMillan PF (1994) Water solubility and speciation models. Mineral Soc Am. Rev Mineral 30:131–152

Merrill RB, Robertson JK, Wyllie PJ (1970) Melting reactions in the system $NaAlSi_3O_8$–$KAlSi_3O_8$–SiO_2–H_2O to 20 kilobars compared with results for other feldspar–quartz–H_2O and rock–H_2O systems. J Geol 78:558–569

Montel JM, Vielzeuf D (1997) Partial melting of metagreywackes, Part II. Compositions of minerals and melts. Contrib Mineral Petrol 128:176–196

Nekvasil H (1988) Calculated effect of anorthite component on the crystallization paths of H_2O-undersaturated haplogranitic melts. Am Mineral 73:966–981

Nekvasil H, Carroll W (1996) Experimental constraints on the compositional evolution of crustal magmas. Trans R Soc Edinb, Earth Sci 87:139–146

Nowak M, Behrens H (1995) The speciation of water in haplogranitic glasses determined by in situ near-infrared spectroscopy. Geochim Cosmochim Acta 59:3445–3450

Patino Douce AE, Johnston AD (1991) Phase equilibria and melt productivity in the pelitic system: implications for the origin of peraluminous granitoids and aluminous granulites. Contrib Mineral Petrol 107:202–218

Patino Douce AE, Beard JS (1994) H_2O loss from hydrous melts during fluid-absent piston-cylinder experiments. Am Mineral 79:585–588

Patino Douce AE, Beard JS (1995) Dehydration melting of biotite gneiss and quartz amphibolite from 3 to 15 kbar. J Petrol 36:707–738

Pichavant (1987) Effects of B and H_2O on liquidus phase relations in the haplogranite system at 1 kbar. Am Mineral 72:1056–1070

Pichavant M, Holtz F, McMillan PF (1992) Phase relations and compositional dependence of H_2O solubility in quartz-feldspar melts. Chem Geol 96:303–319

Scaillet B, Holtz F, Pichavant M (1998) Phase equilibrium constraints on the viscosity of silicic magmas. 1. Volcanic-plutonic comparison. J Geophys Res 103:27257–27266

Schairer JF (1950) The alkali–feldspar join in the system $NaAlSiO_4$–$KAlSiO_4$–H_2O. J Geol 58(5):512–517

Schairer JF, Bowen NL (1935) Preliminary report on equilibrium-relations between feldspathoids, alkali feldspars and silica. Am Geophys Union Trans, 16th Annu Meet, pp 325–328

Shen AH, Keppler H (1995) Infrared spectroscopy of hydrous silicate melts to 1000°C and 10 kbar – direct observation of H_2O speciation in a diamond-anvil cell. Am Mineral 80:1335–1338

Silver L, Ihinger PD, Stolper E (1990) The influence of bulk composition on the speciation of water in silicate glasses. Contrib Mineral Petrol 104:142–162

Springer W, Seck HA (1997) Partial fusion of basic granulites at 5 to 15 kbar: implications for the origin of TTG magmas. Contrib Mineral Petrol 127:30–45

Steiner JC, Jahns RH, Luth WC (1975) Crystallization of alkali-feldspar and quartz in the haplogranite system $NaAlSi_3O_8$–$KAlSi_3O_8$–SiO_2–H_2O at 4 kbar. Geol Soc Am Bull 86:83–98

Stolper E (1982)The speciation of water in silicate melts. Geochim Cosmochim Acta 46:2609–2620

Tamic N, Behrens H, Holtz F (2001) The solubility of H_2O and CO_2 in rhyolitic melts in equilibrium with a mixed CO_2-H_2O fluid phase. Chem Geol 174:333–347

Truckenbrodt J, Johannes W (1999) H_2O loss during piston-cylinder experiments. Am Mineral 84:1333–1335

Tuttle OF, Bowen NL (1958) Origin of granite in the light of experimental studies in the system $NaAlSi_3O_8$–$KAlSi_3O_8$–SiO_2–H_2O. Geol Soc Am Mem 74

Yamashita S (1999) Experimental study of the effect of temperature on water solubility in natural rhyolite melt to 100 MPa. J Petrol 40:1497–1507